Hervas-Blasco, E.; Navarro-Peris, E.; Barceló Ruescas, F.; Corberán, JM. (10-2). Improved water to water heat pump design for low-temperature waste heat recovery based on subcooling control. International Journal of Refrigeration. 106:374-383. https://doi.org/10.1016/j.ijrefrig.2019.06.030

Optimized water to water heat pump design for low-temperature waste heat recovery based on subcooling control

Estefanía Hervás-Blasco[(a)], Emilio Navarro-Peris[(a)], Francisco Barceló-Ruescas[(a)], José Miguel Corberán[(a)]

[(a)] Institut Universitari d'Investigació d'Enginyeria Energètica, Universitat Politècnica de València,

Camí de Vera s/n, València, 46022, Spain

Tel: +34 963879123

enava@ter.upv.es

Abstract

Traditional heat pumps designs have been optimized for heating applications based on small secondary temperature lifts (around 5 K); however, in applications with other characteristic temperature lifts, different design criteria could be required. For instance, transcritical cycles have demonstrated to have a high efficiency for domestic hot water production with high water temperature lifts.

This work presents the experimental results of a new water-to-water heat pump composed by the basic heat pump components (condenser, compressor, evaporator, expansion valve and liquid reliever) able to adapt its performance depending on the required water temperature lift. Domestic hot water production from grey water waste heat recovery has been chosen as experimental application to test this heat pump. Results show COP values up to 5.5 at the design condition (20-15ºC at the inlet-outlet of the evaporator and 10-60ºC at the inlet-outlet of the condenser) and an optimal degree of subcooling of 47K.

Keywords: heat pump; optimal control, water heating, subcooling; superheat

NOMENCLATURE

10K2V: configuration with superheat=10K/two control valves

0K1V: configuration with superheat=0K/one control valve

Tw,ei: water inlet temperature at the evaporator (ºC)

Tw,ci: water inlet temperature at the condenser (ºC)

Tw,co: water outlet temperature at the condenser (ºC)

COP: Coefficient of Performance, [-]

p: Pressure [bar]

Sc: Subcooling, [K]

Sh: Superheat [K]

T: Temperature [ºC]

Greek symbols

Δ: Variation

Subscripts

comp: Compressor

cond: Condenser, or gas cooler

evap: evaporator

in: inlet

opt: Optimal

out: Outlet

ref: Refrigerant

1. INTRODUCTION

Looking for a decarbonized energy sector, the use of renewable energies as well as efficient technologies arise as focus for next decades, where a change on the energy system is required (García-Álvarez et al., 2016).

Heat pumps (HP) are a mature technology widely used due to its high performance, reliability and stability. Nowadays, they are on growing interest as alternative to conventional water heating systems (boilers, solar thermal) as the European Directive 2009/28/CE recognizes the water heated with a HP able to operate with a Seasonal Performance Factor (SPF) greater than 2.5 as if it was produced by renewable energies ("DIRECTIVE 2009/28/EC OF THE EUROPEAN PARLIAMENT AND OF THE COUNCIL" of 23 April 2009 on the promotion of the use of energy from renewable sources and amending and subsequently repealing Directives 2001/77/EC and 2003/30/EC).

As demonstrated in other works, their efficiency strongly depends on the external conditions (Pitarch et al., 2017a). Domestic Hot Water (DHW) applications deal with high secondary temperature lifts at the condenser, the tap water is around 10ºC and needs to be heated up to at least 60ºC, contrary to the most widespread applications of HP until the moment (heating and cooling applications with low temperature lifts at the secondary fluids) (Cecchinato et al., 2005a; Zehnder, 2004). Thus, HPs for DHW applications are still a field with room for improvement (Gunerhan et al., 2014).

Furthermore, new heat recovery applications, based on low-grade temperature mass flows currently wasted to the ambient such as heat recuperation from the sewage in residential sector or from condensing loops in commercial/industrial sectors, are gaining importance within HPs. This heat, usually at temperature slightly higher than the ambient, becomes a valuable and stable heat source in HPs that are able to elevate the temperature of the heat sink up to useful levels. Hence, high or at least different temperature lifts at the secondary fluid in the evaporator may also take place, which is a new topic that needs further research and understanding (Law et al., 2013; David et al., 2017; Meggers and Leibundgut, 2010; Cipolla and Maglionico, 2014; Shen et al., 2018).

Another issue related to HPs is the working fluid (refrigerant). In order to meet all the characteristics required, that is, good thermodynamic properties, safety and environmentally friendly, natural refrigerants (carbon dioxide –CO2 (R744), hydrocarbons (HCs) and ammonia (NH3)) are seen as the solution for now and the next future (Lorentzen, 1995; Ajuka et al., 2017).

According to the above mentioned, a research line from the last and the coming years is the study and integration of heat recovery heat pumps (HRHPs) working with natural fluids for DHW production (To, 2013) .

Among the cited refrigerants, transcritical cycles (CO2) present higher efficiency than subcritical with high temperature lifts due to a better match of the temperature profile between the secondary and the refrigerant in the condenser side (Stene, 2007; Cecchinato et al., 2005a; Yokoyama et al., 2010). For that reason, CO2 has been the most used refrigerant in DHW applications ("Eco Cute | MAYEKAWA Global (MYCOM)," 2009; Nekså et al., 1998; Nekså, 2002; Cecchinato et al., 2005b). However, subcritical refrigerants have also been used to this purpose. In these cases, to avoid the loss of efficiency, the heating process is progressive and divided in steps of around 5K until it reaches values up to 60ºC (Quantum National Distributor, 2018).

Recently, researches have been dealing with the study of the benefit obtained from the application of a certain degree of subcooling in subcritical cycles (Pitarch et al., 2017b; Pitarch et al., 2018; Alonso and Stene, 2010; Pottker and Hrnjak, 2015) in order to adapt the performance of the system to the required water temperature lift. With subcooling, a better temperature profile match between the secondary fluid and the subcritical cycle is possible. Thus, improving the efficiency of the heating process. While the existence of an optimal active charge of the system (directly related to the condenser subcooling) was studied in the past (Cecchinato et al., 2005b; Corberán et al., 2008), it was mainly for applications with low water temperature lifts and the optimal subcooling was found in the interval of 5-10K only for the nominal condition. But as it has been demonstrated by Pitarch et al., (2017a), these results depend not only on the heat pump design but also on the target application. For

instance, for an application with a temperature lift in the condenser of 50K the optimal degree of subcooling has been found to be around 43K and the obtained improvement for these conditions from working at 0 K of subcooling was 31% in terms of COP.

In this way, subcritical cycles working with the optimal degree of subcooling and high temperature lifts are able to operate under similar efficiencies than transcritical cycles and their design is more flexible to different operating conditions (Pitarch et al., 2017b).

The same approach could be extrapolated to the evaporator side, where superheat was only applied to ensure the reliability of the compressor, in that sense usually it has been considered as harmful and only recommendations of 5-10K are given (Jolly et al., 2001). This point may become important within heat recovery applications.

Derived from all of the above, a heat pump system needs to have a proper control strategy that allows the adaptation to the external conditions in order to operate under the maximum performance (Stene, 2007). To that purpose, different control strategies have been used: from the analysis of the operational parameters and degrees of freedom (Kim et al., 2004; Jensen and Skogestad, 2007) to complex algorithms (Koeln and Alleyne, 2014; Hu et al., 2015) based on seeking control or to simpler controls based on the temperature approach as assessed by Hervas-Blasco et al., (2018).

In this work, a new heat pump prototype with the same components of a standard heat pump has been build. The heat pump uses the expansion valve to control subcooling instead of superheat. Superheat is fixed to 0 K placing the liquid receiver at the outlet of the evaporator. With that configuration, the heat pump is able to adapt its subcooling to the external condenser conditions resulting in an improvement of the COP without adding any additional cost to a regular system. The prototype has been tested for an application of domestic hot water production with heat recovery from the sewage water. Later, the results have been compared with the results obtained in the heat pump presented by Pitarch et al., (2018) which has been especifically designed for that target. That heat pump has been considered as the reference one as it was able to control the subcooling and the superheat

independently but introducing more components in the system. Derived from that, the selected refrigerant was propane (the one used in the reference system), although the results can be generalized for other refrigerants.

2. HEAT PUMP DESIGN

The developed prototype is a water-to-water heat pump (WtWHP) for heating water from 10ºC -60ºC from the heat recovery of any low temperature water source which controls the subcooling with the expansion valve in order to maximize the efficiency.

Figure 1 shows the lay-out and the refrigerant cycle of the prototype 0K1V (zero superheat, one valve).

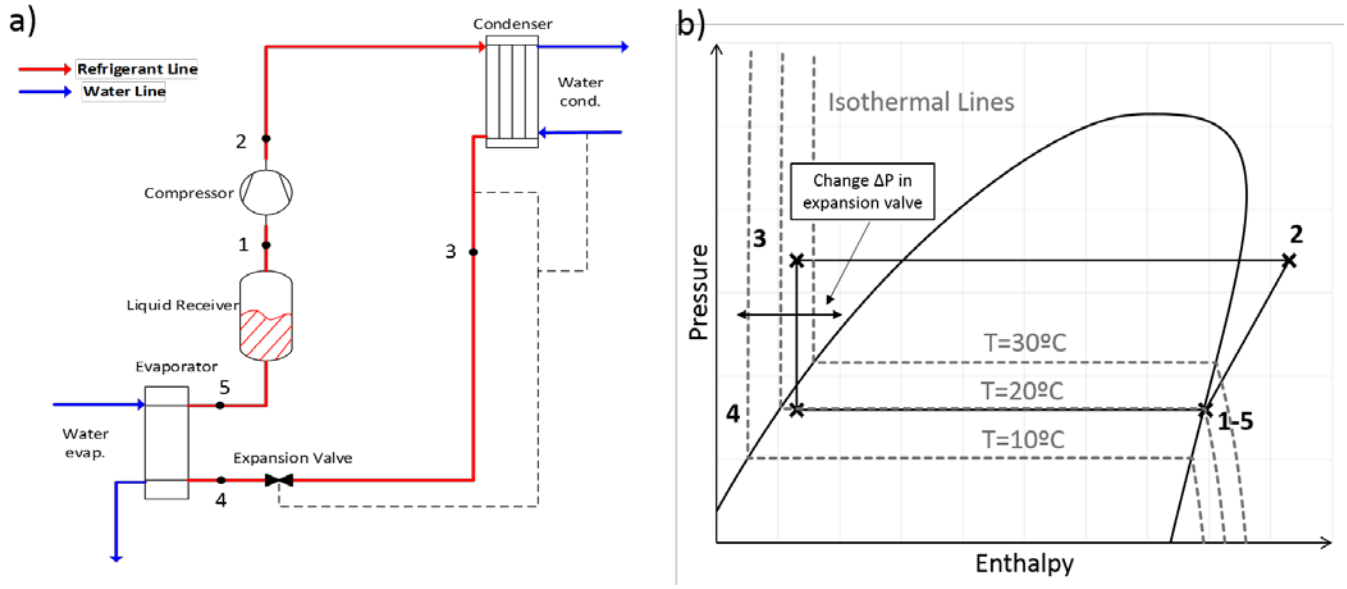

Figure 1: 0K1V configuration (a) system lay-out (b) refrigerant cycle

The objective of testing this configuration is to analyze the reliability and stability of this system that has the same components as a typical heat pump but the expansion valve (thermostatic or electronic) is dedicated to the subcooling control at the expense of losing the superheat control. In this sense, the liquid receiver is placed at the outlet of the evaporator (point 5) ensuring saturated vapor conditions (zero superheat). The evaporation pressure depends mainly on the heat process at the evaporator (points 4-5) while the condensing pressure is constrained from the heat process in the condenser

(points 2-3). The pressure drop introduced by the expansion valve will determine the degree of subcooling made at the condenser. Hence, lower degrees of subcooling are obtained. In this configuration, a liquid-suction heat exchanger may be suitable for other applications where the temperature at the outlet of the condenser is not too close to the evaporation temperature. The control strategy implemented in the system is based on the temperature approach measurement following the same approach as the one performed by Hervas-Blasco et al., (2018). Please refer to it for further details.

Some aspects would need to be carefully addressed:

1. Control reliability: even though this configuration has been used with transcritical cycles before, the characteristics of both type of cycles are significantly different and the reliability and stability of the proposed heat pump must be tested. In transcritical cycles, the control of the rejection pressure by means of the drop pressure in the expansion valve is accurate and stable. However, in this case the pressure drop in the valve is going to control a temperature difference, therefore, at the beginning of this work it was unknown if this kind of control would be reliable.
2. Liquid receiver: stability and reliability problems associated to the deposit placed at the inlet of the compressor could appear.
3. Not superheat control penalty: in common heat pump applications, superheat has a negative impact on the efficiency. However, within heat recovery applications, were large secondary temperature lifts at the evaporator take place, certain degree of superheat could constitute a benefit, as it will allow the increase of the evaporating pressure. Therefore, work at 0 K superheat could constitute a penalty to the efficiency of this design that must be evaluated.

The implemented control algorithm was based on the temperature difference between the water inlet temperature and the refrigerant outlet temperature in the condenser used by Hervas-Blasco et al., (2018). Vapor conditions at the inlet of the compressor are ensured by placing a sight glass at the

outlet of the liquid receiver and by removing part of the isolation in the circuit from the liquid receiver to the compressor.

Finally, the analysis of the impact on the efficiency due to the lack of superheat and its control has been addressed by comparing the experimental results to the results obtained for a HP configuration in which both, subcooling and superheat control, are possible at the expense of an extra valve. This system is referred as 10K2V and will work at 10 K of superheat. Further details of the last configuration can be found in the work by Pitarch et al., (2016).

3. EXPERIMENTAL SETUP AND TEST PROCEDURE

3.1. Test rig

Figure 2 shows a general lay-out of the HP test rig. The rig allows the control of the water temperatures at the condenser (points 1-2) that simulate the heat sink and at the evaporator (points 3-4) simulating the water recovery mass flow.

The heat pump prototype has been designed to obtain around 50kW at the design point (20-15ºC at the water inlet-outlet evaporator and 10-60ºC at the water inlet-outlet condenser) and the test rig is capable to test HPs up to 70kW.

The heat pump itself is placed inside the black dotted points and the circuit of the 0K1V is represented in red. The test rig used is the same as the one used by Pitarch et al., (2016), please refer to it for a more detailed explanation. For further details on the sensors and the instrumentation used including the error analysis, please refer to the publication by Pitarch et al., (2018). The total uncertainty for

COP and heating capacity is lower than ±0.08 and ±0.05 kW, respectively, for all measurements.

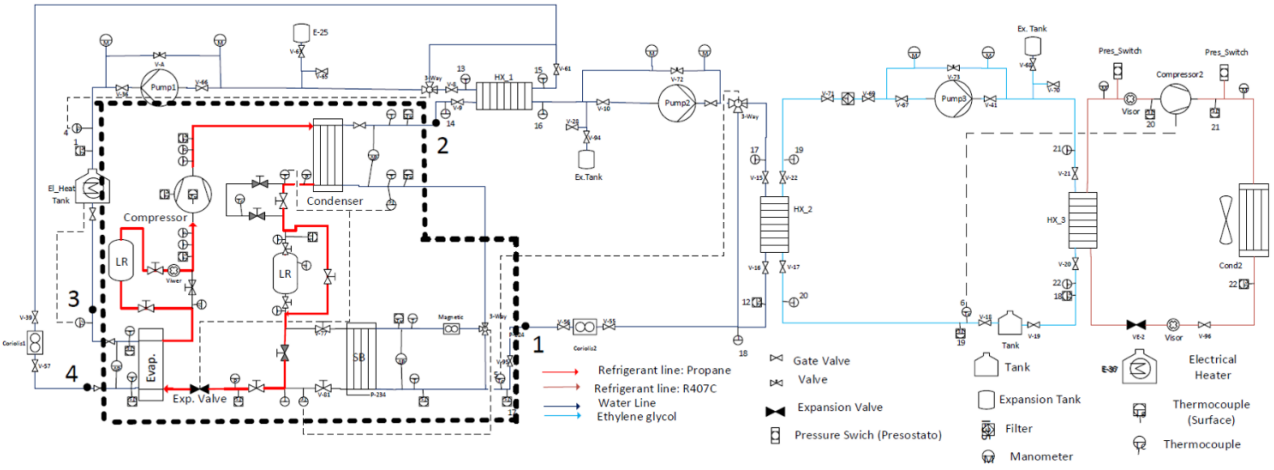

Figure 2: Overview of the HP test rig and sensors used in the experimental setup.

Table 1 shows the characteristics of the main components used in the prototype and the configuration. The same size of the components as the reference case (10K2V) has been chosen in order to obtain comparable results.

Table 1: Characteristics of the components of the HP system

Component	Type	Size
Compressor	Scroll (2900rpm)	29.6m^3h^{-1}
Condenser	BPHE Counter-flow	3.5m2
Evaporator	BPHE Counter-flow	6m2
Liquid receiver	-	8 l
Expansion valve	Electronic EV	5-60kW

3.2 Sensors and error analysis

The evaporator and condenser capacities of the heat pump were measured in the water side. In order to measure them as accurate as possible, six RTDs were located at inlet/outlet of each heat exchanger directly in contact with the water. To monitor and measure temperature in other points, a total number

of 27 T-type thermocouples were used. The water mass flow through evaporator and condenser were measured with Coriolis mass flow meters. For the pressure, at the refrigerant side there were two pressure transducers. In the water side, there were 3 differential pressure sensors to measure the pressure drop in the heat exchangers. With these measurements and according to the norm EN 14511-3 "Test methods" (DIN EN 14511-3, 2013), the auxiliary consumption of the water pumps was calculated.

Table 2 shows these sensors with the relative and absolute accuracy for each sensor. From these sensors and the characteristics of the experimental set up the total uncertainty of the variables not measured directly like COP and heating capacity does not overpass ±0.08 and ±0.05 kW respectively for all measurements.

Magnitude	Model	Relative Accuracy	Absolute Accuracy	Units
Pressure	Differential 1151 Smart Rosemount	0.13 % of Span	5 E-04	bar
	Differential p Siemens Sitrans	0.14 % of Span	4 E-04	bar
	Differential p Setra	0.3 % of Span	1.7 E-03	bar
	P 1151 Smart GP7 Rosemount	0.12 % of Span	0.03	bar
	P 1151 Smart GP8 Rosemount	0.15 % of Span	0.08	bar
Temperature	Thermocouple T Type		1	ºC
	RTD Class 1/10 DIN		0.06	ºC
Flow	Coriolis SITRANS F C MASS 2100	0.3 % of Reading		
Power	DME 442	0.3 % of Reading		

Table 2: Sensors and their uncertainty

3.3. Experimental campaign

The experimental campaign is divided in three parts:

1. **Reference conditions**: A campaign including a total of 86 measurements, where most of the common DHW and the heat recovery water temperatures have been covered through it. 60ºC has been set as the condenser outlet temperature of the water. The inlet water temperature at the condenser varies from 10ºC-50ºC. The water inlet conditions at the evaporator range from 10ºC to 30ºC representing the temperature of the water in the sewage or a heat recovery process. The water mass flow rate in the evaporator was adjusted in the nominal point and it is kept constant for the rest of the test points (~7000kg/h), this procedure is described in the European Standard EN 14825. Superheat is kept always lower than 2K.

   Table 2 collects the matrix of the conditions tested with 0K1V prototype.

Table 2: Experimental campaign matrix with 86 measurements carried out in the OK1V configuration

$T_{in\_water\_evap}$ [ºC]	$T_{in\_water\_cond}$[ºC]	$T_{out\_water\_cond}$[ºC]	Refrigerant subcooling range [K]
10	10	60	4 to 54
	30		4 to 36
	50		4 to 16
20	10		4 to 54
	30		4 to 36
	50		4 to 16
30	10		4 to 54
	30		4 to 36
	50		4 to 16

2. **Water heating limit conditions**: to test the capabilities of the prototype, 16 new measurements considering higher outlet temperatures at the condenser were performed for the OK1V prototype. In order to be able to compare the obtained results with the reference the same test campaign was repeated for 10K2V prototype.

Table 3 shows the matrix of the conditions tested with both configurations for different water temperatures at the outlet of the condenser.

Table 3: Experimental campaign matrix with 16 measurements carried out in the OK1V and 10K2V configurations

$T_{in\_water\_evap}$ [ºC]	$T_{in\_water\_cond}$[ºC]	$T_{out\_water\_cond}$[ºC]
20	30	70
		80
		90
20	40	80
		90
30	30	70
		80
		90

3. **Evaporator conditions**: An experimental campaign of 54 measured points was performed in order to study the optimal water mass flow rate through the evaporator (optimum DT). This campaign supplies very relevant information in order to understand the system behavior for energy recovery applications. As in the previous cases, the test campaign was performed for the analyzed prototype 0K1V and the reference system 10K2V.

Table 4 shows the matrix of the conditions tested with both configurations in order to obtain the optimal water mass flow rate through the evaporator.

Table 4: Experimental campaign matrix with 54 measurements carried out in the OK1V and 10K2V configurations

$T_{in\_water\_evap}$ [ºC]	D_{Tevap} [K]	$T_{in\_water\_cond}$-$T_{out\_water\_cond}$[ºC]	Refrigerant subcooling range [K]
15	3.5-9	20-60	28-39
20	4-12.5		
35	5-21		

4. RESULTS

4.1. Reference conditions.

This section presents the experimental results obtained from the reference conditions campaign collected in Table 2 and the 0K1V prototype. In order to directly compare the results with the reference system (prototype in which both controls are possible), the experimental results obtained with the 10K2V prototype presented previously by Pitarch et al., (2018) have been included also here Figure 3 shows the heating COP variation with subcooling obtained for both configurations at different water temperature conditions. (a) Evaporator water inlet temperature of 10°C, (b) Evaporator water inlet temperature of 20°C and (c) Evaporator water inlet temperature of 30°C. 10K2V configuration is represented by dots while 0K1V configuration by triangles. Filled markers belong to 0K1V and not filled markers to the reference prototype, 10K2V. Triangles represent the condenser water temperature (10-60ºC), dots the water temperature at the condenser (30-60ºC) and squares markers to (50-60ºC).

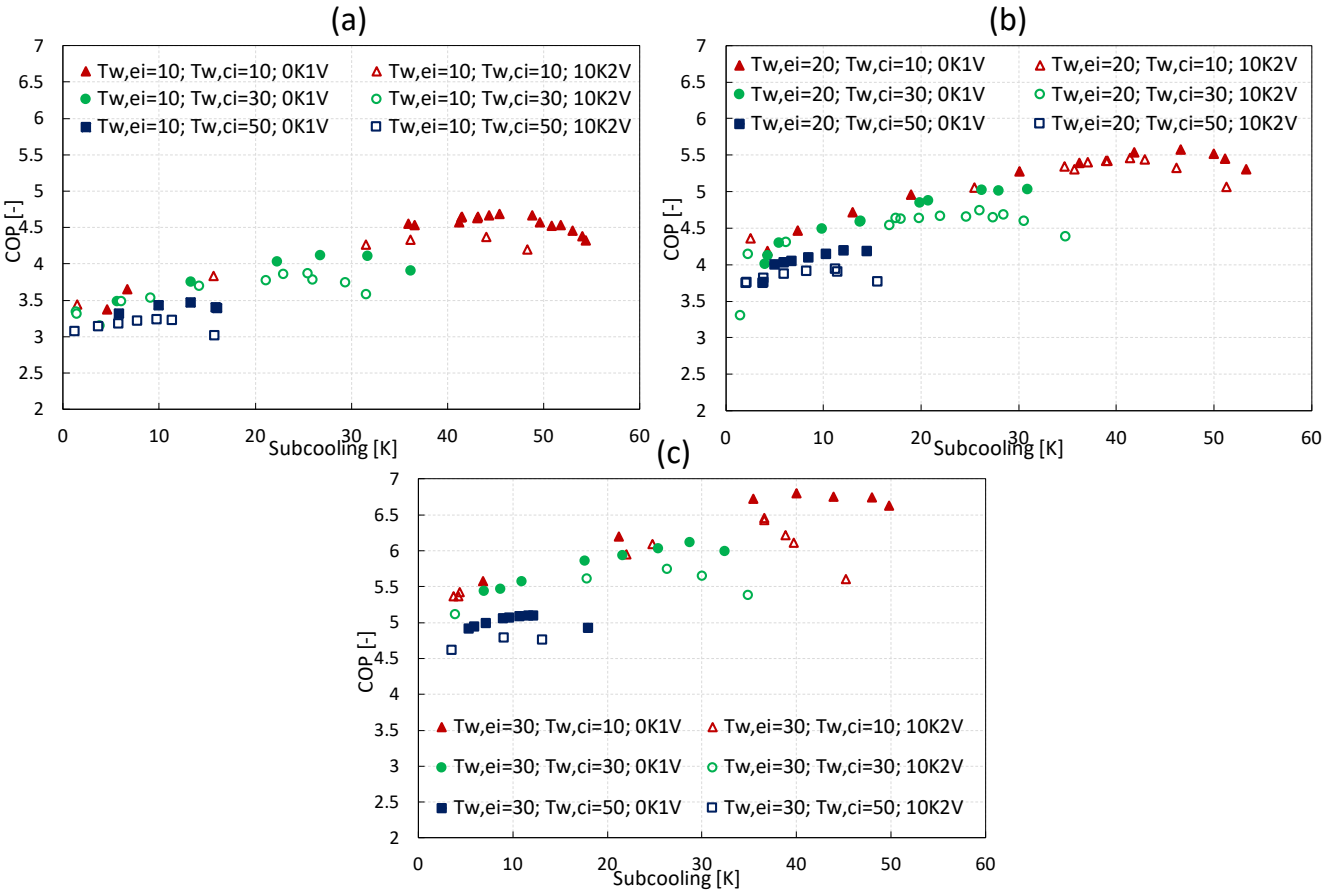

Figure 3: Heating COP variation with subcooling at different temperatures for both configurations and (a) Tevap_water_inlet=10°C (b) Tevap_water_inlet=20°C and (c) Tevap_water_inlet=30°C.

According to Figure 3:

1. The heating COP increases as the evaporating temperature and the water temperature lift at the condenser are higher.
2. The heating COP at the design point (20ºC at the evaporator water inlet temperature and 10-60ºC at the condenser) is 5.58 (2% higher than the one obtained with 10K2V). The application of the optimal degree of subcooling improves the efficiency up to 25% with regards not having subcooling
3. An optimal subcooling based on the water temperature lift at the condenser is obtained. The optimal subcooling is around 5K higher in the 0K1V configuration than in the 10K2V configuration.
4. The optimal subcooling was obtained for approximately the same temperature difference between the refrigerant temperature at the outlet of the condenser and water temperature at the inlet of the condenser of the obtained for the reference system. This result is very relevant from the point of view of developing a commercial prototype as allows a very simple control strategy in order to work in the optimum subcooling.
5. The COP of 0K1V, is greater than the one obtained with the 10K2V at any condition.
6. The 0K1V has a lower reduction in COP as a consequence of working at higher subcoolings than the optimums obtained for the10K2V system.

Figure 4 represents the suction and discharge pressures of the system for both prototypes with subcooling at different water temperature conditions (a) Evaporator water inlet temperature of 10°C, (b) Evaporator water inlet temperature of 20°C and (c) Evaporator water inlet temperature of 30°C. 10K2V configuration is represented by dots while 0K1V configuration by triangles. Filled markers belong to 0K1V and not filled markers to the reference prototype, 10K2V. Triangles represent the condenser water temperature (10-60ºC), dots to (30-60ºC) and squares markers to (50-60ºC).

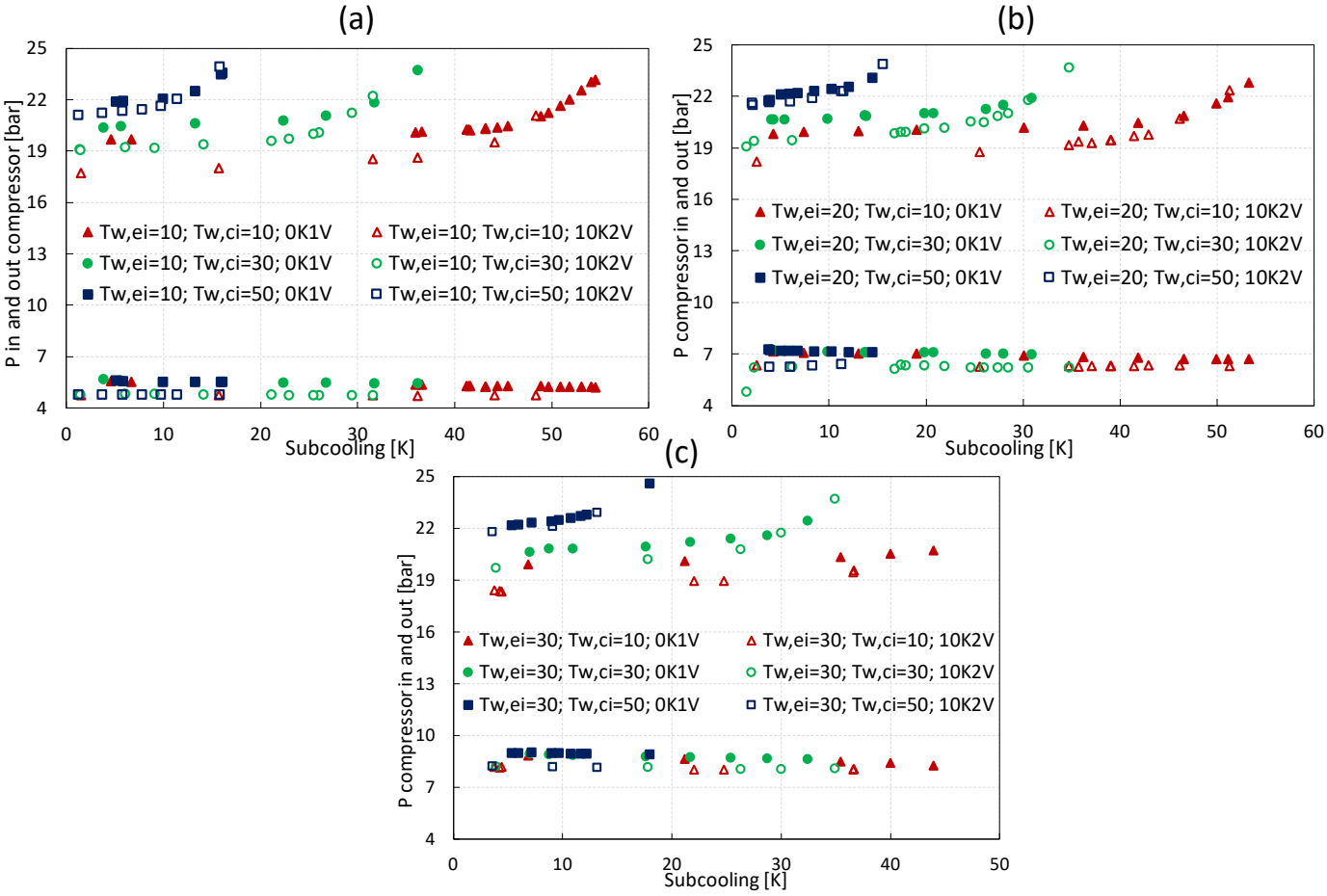

Figure 4: Compressure suction and discharge pressure variation with subcooling at different water temperatures for the 0K1V and the 10K2V configurations. (a) Tevap_water_inlet=10°C (b) Tevap_water_inlet=20°C and (c) Tevap_water_inlet=30°C.

Form Figure 4 the following comparative behavior is extracted:

1. The evaporating pressure remains similar within the same water inlet temperature at the evaporator regardless the subcooling conditions. The 0K1V has a slightly higher evaporation temperature than the 10K2V.
2. The 0K1V configuration works with slightly higher pressures than the 10K2V configuration (due to the fact of having higher subcooling). This effect becomes more important as the temperature lift in the condenser decreases and the water inlet temperature at the condenser increases.
3. The discharge pressure remains almost constant before the optimal subcooling and it is higher in the 0K1V configuration, especially when high water temperature lifts in the condenser take

place (because of zero superheat, higher pressures are attained becoming a penalty for the 0K1V configuration if working with lower subcooling than the optimal). Once the optimal subcooling is reached, the discharge pressure exponentially increases not presenting significant differences between both configurations.

Figure 5 represents the compressor discharge temperature for both prototypes as a function of subcooling at different water temperature conditions (a) Evaporator water inlet temperature of 10°C, (b) Evaporator water inlet temperature of 20°C and (c) Evaporator water inlet temperature of 30°C. 10K2V configuration is represented by dots while 0K1V configuration by triangles. Filled markers belong to 0K1V and not filled markers to the reference prototype, 10K2V. Triangles represent the condenser water temperature (10-60ºC), dots to (30-60ºC) and squares markers to (50-60ºC).

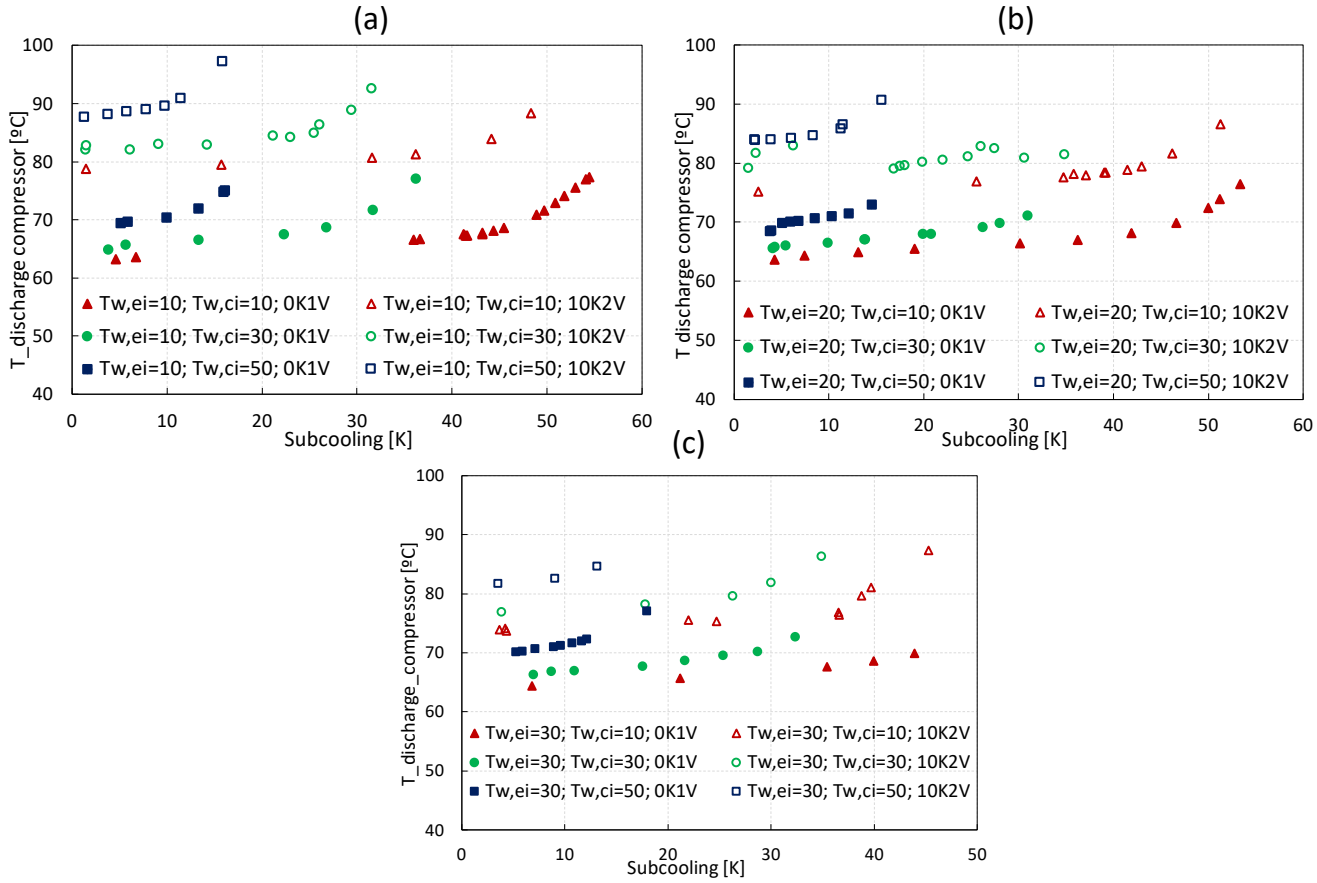

Figure 5: Discharge temperature variation with subcooling at different water temperatures for the 0K1V and the 10K2V configurations. (a) Tevap_water_inlet=10°C (b) Tevap_water_inlet=20°C and (c) Tevap_water_inlet=30°C.

As it can be seen in Figure 5, the discharge temperature is always around 10K lower in the 0K1V than in 10K2V. This is a direct consequence of the superheat degree and lead to obtain higher optimal degrees of subcooling in 0K1V.

For water heating applications, lower discharge temperatures lead to higher condensing temperatures in order to obtain the same water outlet temperatures. This effect will have a significant influence especially for high water temperatures such as 80-90ºC. Thus, it is analyzed more in deep later on.

3.2.Water heating limit conditions:

Figure 6 represents the heating COP for the prototype as function of the water temperature in the condenser outlet at different water temperature conditions compared to the reference system. 10K2V is represented by dots while 0K1V by line markers. Red color belongs to evaporator water inlet temperature of 20ºC and condenser water temperature of 30ºC, green color to 20ºC at the inlet of the evaporator and 40ºC at the inlet of the condenser and black color 30ºC evaporator and 30ºC condenser inlet water temperature.

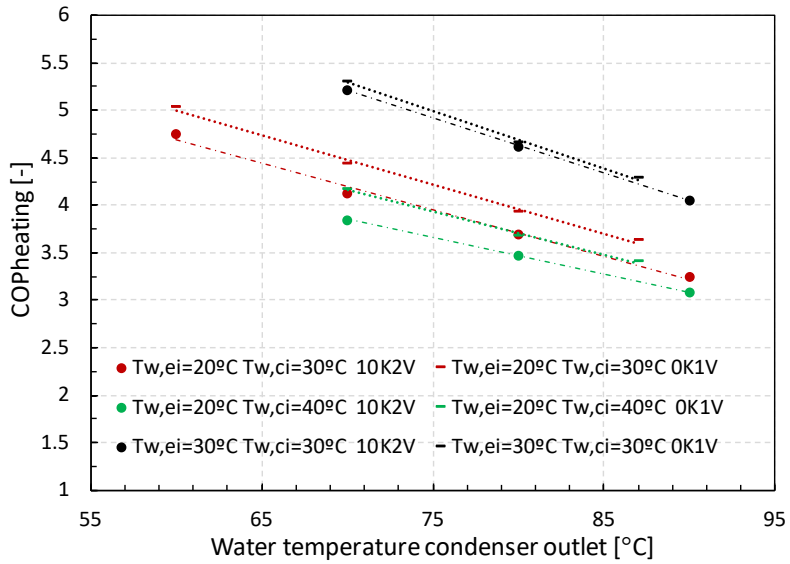

Figure 6: COP heating as a function of Tw,co for different water conditions at the inlet of the condenser and evaporator in both configurations.

As it can be seen in Figure 6, the same results are obtained with the increase of the water outlet temperature at the condenser, that is, the 0K1V maintain its better performance for all the conditions. However, it is worth it to remark that 90ºC were impossible to attain with the 0K1V configuration being the maximum stable temperature 87ºC due to the increase of the discharge pressure was close to the propane critical point.

Figure 7 represents discharge pressure for 0K1V as function of the water temperature in the condenser outlet at different water temperature in the condenser inlet conditions compared to the reference state. 10K2V is represented by dots while 0K1V by lines markers. Red color belongs to evaporator water inlet temperature of 20ºC and condenser water temperature of 30ºC, green color to 20ºC at the inlet of the evaporator and 40ºC at the inlet of the condenser and black color 30ºC evaporator and 30ºC condenser inlet water temperature.

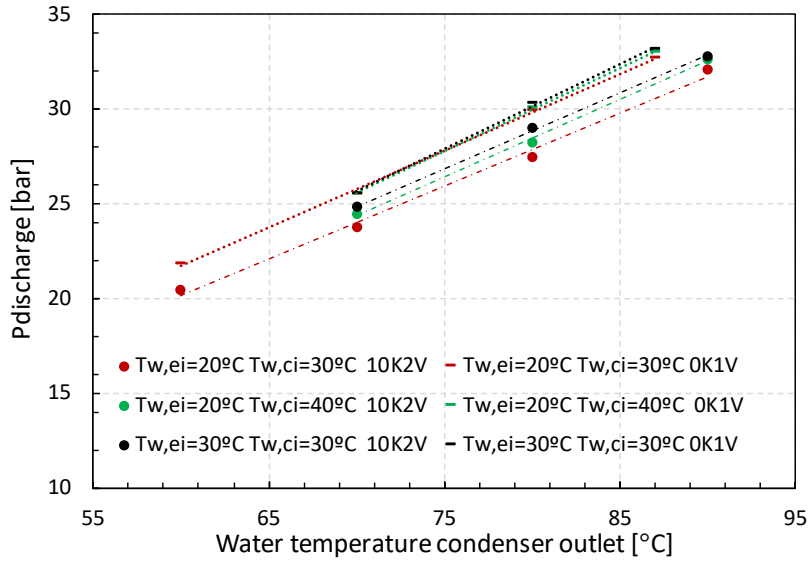

Figure 7: Discharge pressure as a function of Tw,co for different water conditions at the inlet of the condenser and evaporator in both prototypes.

According to the figure, the discharge pressure of 0K1V is always greater than the one reached with the 10K2V. This fact limits the maximum stable temperature for 0K1V system.

This effect may limit the application of the new configuration to DHW since to heat water up to 80-90ºC results in a very high discharge pressure.

4.3. 3. Evaporator conditions

Figure 8 shows the COP heating for both prototypes as a function of the evaporator water temperature lift for different water inlet temperatures at the evaporator and 40K of water temperature lift at the condenser (20-60ºC). Triangles belong to the 0K1V configuration and circles to the 10K2V. Black color is used for Tw,ei=35ºC, red color configuration for Tw,ei=20ºC and green color for Tw,ei=15ºC.

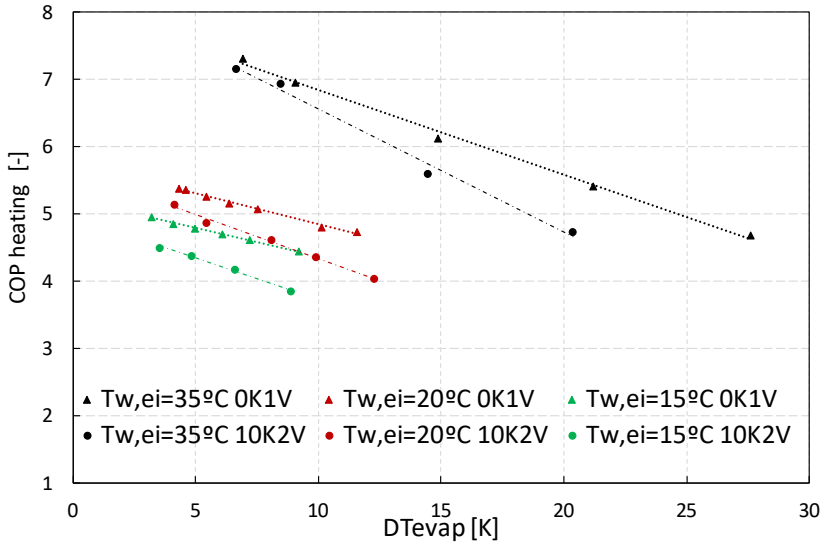

Figure 8: Heating COP variation with the water temperature lift at the evaporator. Tw,ci=20˚C and Tw,co=60 ˚C and different Tw,ei for 0K1V and 10K2V configurations.

According to Figure 8, it seems that the higher the mass flow, the higher the COP heating is. Hence, for the tested water mass flows, one would always use the maximum. However, it is expected that at some point, the auxiliaries would penalize more and a maximum would be found. This analysis has not been experimentally performed since the water pumps available on the test bench were not able to handle higher mass flows.

Furthermore, as it can be seen, the performance is always greater in the 0K1V regardless the water mass flow rate through the evaporator. This difference becomes more significant as the water mass flow diminishes (greater DTevap). This result is the opposite of the expected from theoretical considerations as for high DTevap having superheat should increase the evaporating temperature which would benefit the configuration with superheat (Pitarch et al.2019). According this assumption, the prototype 0K1V should show a better performance for low DTevap level but as DTevap increases the difference should be reduced up to a value were the reference system 10K2V should show a better COP.

Figure 9 represents (a) the suction pressure (related to the evaporating pressure) and (b) the compressor inlet temperature (related to the evaporating temperature taking into account the superheat in 10K2V) function of the water temperature lift at the evaporator for different water inlet temperatures at the evaporator and 40K of water temperature lift at the condenser (20-60ºC). Triangles belong to the 0K1V configuration and circles to the 10K2V. Black color is used for Tw,ei=35ºC, red color configuration for Tw,ei=20ºC and green color for Tw,ei=15ºC.

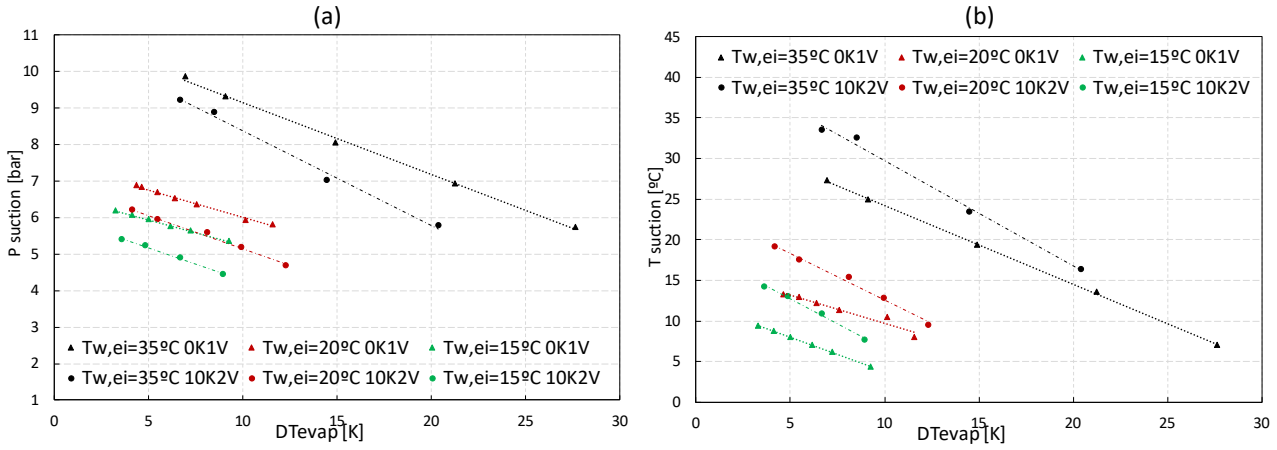

Figure 9: (a) Suction pressure and (b) Suction temperature variation with the water temperature lift at the evaporator. Tw,ci=20˚C and Tw,co=60 ˚C and different Tw,ei for 0K1V and 10K2V configurations.

According to Figure 9, the evaporating pressure has the same trend as the performance, the difference between the 0K1V and 10K2V becomes more important as DTevap increases. As it has been

commented previously, it would be expected that high water temperature lifts penalize the evaporator by reducing the evaporating pressure compared to the 10K2V. However, this behavior is not observed. A possible explanation for that could be related with the different vapor qualities at the inlet of the evaporator which could induce bad refrigerant distribution within the evaporator. Nevertheless, further investigation is required in order to find an explanation for the obtained results.

5. CONCLUSIONS

This paper presents the performance of a new water-to-water heat pump which improves the performance of the system using the expansion valve to control the subcooling instead of the superheat. The heat pump developed has been systematically compared with a heat pump which is able to control the superheat and the subcooling showing higher performance for all the tested conditions.

From all the results, these main conclusions can be extracted:

1. The 0K1V configuration is stable and does not present control problems.
2. The 0K1V configuration without superheat has greater performance than the 10K2V configuration for all the tested conditions. The improvement is around 5% .
3. Comparing the 0K1V prototype with the reference 10K2V, the proposed system has higher discharge pressures, around 10K lower discharge temperatures and the optimal subcooling is around 5K greater. However, the reference system (10K2V) is able to reach higher water temperatures at the outlet of the condenser which could limit the application range of the 0K1V.
4. This limitation factor for the 0K1V could be solved including a liquid to suction heat exchanger after the receiver. Nevertheless, to make it effective, it should be checked that the temperature difference between the evaporator and the condenser is high enough and that it could be cost effective as an additional element is being introduced.

5. The optimum subcooling is found for a temperature difference between the refrigerant outlet and the water inlet in the condenser of 3K for both systems, therefore, to use a control strategy of a constant DT at the outlet of the condenser is reliable. This is a very important fact from the point of view of developing a commercial prototype as it will allow the use of electronic expansion valves as well as thermostatic expansion valves.
6. The evaporating pressure is slightly higher in the 0K1V configuration. The vapor quality at the inlet of the evaporator is lower which allows the evaporating pressure to vary only slightly.
7. The application of superheat at the outlet of the evaporator experimentally always penalizes the performance, contrary to the expected from a theoretical analysis. This result is experimentally obtained but further studies are required in order to be able to explain the discrepancy with the expected.

The obtained results show that the proposed heat pump configuration with the proposed control system for the expansion valve could increase significantly the efficiency of the heat pump overall when a high water temperature lift is imposed by the application. Although in the present paper the application has been mainly focused in domestic hot water production, based on the wide test matrix used which has not been limited to a water temperature lift of 50K, the proposed system with the obtained conclusions can be applied to any other application.

ACKNOWLEDGEMENTS

Part of the results of this study were developed in the mainframe of the FP7 European project ‘Next Generation of Heat Pumps working with Natural fluids’ (NxtHPG). Part of the work presented was carried out by Estefanía Hervás Blasco with the financial support of a PhD scholarship from the Spanish government SFPI1500X074478XV0. The authors would like also to acknowledge the Spanish ‘MINISTERIO DE ECONOMIA Y COMPETITIVIDAD’, through the project "MAXIMIZACION DE LA EFICIENCIA Y MINIMIZACION DEL IMPACTO AMBIENTAL DE BOMBAS DE CALOR PARA LA DESCARBONIZACION DE LA CALEFACCION/ACS EN LOS

EDIFICIOS DE CONSUMO CASI NULO" with the reference ENE2017-83665-C2-1-P for the given support.

REFERENCES

Ajuka, L., Odunfa, M., Ohunakin, O., Oyewola, M., 2017. Energy and exergy analysis of vapour compression refrigeration system using selected eco-friendly hydrocarbon refrigerants enhanced with tio2-nanoparticle. Int. J. Eng. Technol. 6, 91. https://doi.org/10.14419/ijet.v6i4.7099

Alonso, M., Stene, J., 2010. IEA heat pump program annex 32 umbrella report: system solutions, design guidelines, prototype system and field testing-Norway, Tech. rep.

Cecchinato, L., Corradi, M., Fornasieri, E., Zamboni, L., 2005a. Carbon dioxide as refrigerant for tap water heat pumps: A comparison with the traditional solution. Int. J. Refrig. 28, 1250–1258. https://doi.org/10.1016/j.ijrefrig.2005.05.019

Cecchinato, L., Corradi, M., Fornasieri, E., Zamboni, L., 2005b. Carbon dioxide as refrigerant for tap water heat pumps: A comparison with the traditional solution. Int. J. Refrig. 28, 1250–1258. https://doi.org/10.1016/j.ijrefrig.2005.05.019

Cipolla, S.S., Maglionico, M., 2013. Heat recovery from urban wastewater: Analysis of the variability of flow rate and temperature. Energy Build. 69, 122–130. https://doi.org/10.1016/j.enbuild.2013.10.017

Corberán, J.M., Martínez, I.O., Gonzálvez, J., 2008. Charge optimisation study of a reversible water-to-water propane heat pump. Int. J. Refrig. 31, 716–726. https://doi.org/10.1016/j.ijrefrig.2007.12.011

David, A., Mathiesen, B.V., Averfalk, H., Werner, S., Lund, H., 2017. Heat Roadmap Europe: Large-scale electric heat pumps in district heating systems. Energies. https://doi.org/10.3390/en10040578

DIRECTIVE 2009/28/EC OF THE EUROPEAN PARLIAMENT AND OF THE COUNCIL of 23 April 2009 on the promotion of the use of energy from renewable sources and amending and

subsequently repealing Directives 2001/77/EC and 2003/30/EC, n.d.

Eco Cute | MAYEKAWA Global (MYCOM) [WWW Document], 2009. URL http://www.mayekawa.com/products/features/eco_cute/

García-Álvarez, M.T., Moreno, B., Soares, I., 2016. Analyzing the sustainable energy development in the EU-15 by an aggregated synthetic index. Ecol. Indic. 60, 996–1007. https://doi.org/10.1016/j.ecolind.2015.07.006

Gunerhan, H., Ekren, O., Araz, M., Biyik, E., Hepbasli, A., 2014. A key review of wastewater source heat pump (WWSHP) systems. Energy Convers. Manag. 88, 700–722. https://doi.org/10.1016/j.enconman.2014.08.065

Hervas-Blasco, E., Pitarch, M., Navarro-Peris, E., Corberán, J.M., 2018. Study of different subcooling control strategies in order to enhance the performance of a heat pump. Int. J. Refrig. https://doi.org/10.1016/J.IJREFRIG.2018.02.003

Hu, B., Li, Y., Cao, F., Xing, Z., 2015. Extremum seeking control of COP optimization for air-source transcritical CO2 heat pump water heater system. Appl. Energy 147, 361–372. https://doi.org/10.1016/j.apenergy.2015.03.010

Jensen, J.B., Skogestad, S., 2007. Optimal operation of simple refrigeration cycles. Comput. Chem. Eng. 31, 712–721. https://doi.org/10.1016/j.compchemeng.2006.12.003

Jolly, P.G., Tso, C.P., Chia, P.K., Wong, Y.W., 2001. Intelligent control to reduce superheat hunting and optimize evaporator performance in container refrigeration, in: ASHRAE Transactions. p. 267. https://doi.org/10.1080/10789669.2000.10391261

Kim, M.H., Pettersen, J., Bullard, C.W., 2004. Fundamental process and system design issues in CO2 vapor compression systems. Prog. Energy Combust. Sci. https://doi.org/10.1016/j.pecs.2003.09.002

Koeln, J.P., Alleyne, A.G., 2014. Optimal subcooling in vapor compression systems via extremum seeking control: Theory and experiments. Int. J. Refrig. 43, 14–25.

https://doi.org/10.1016/j.ijrefrig.2014.03.012

Law, R., Harvey, A., Reay, D., 2013. Opportunities for low-grade heat recovery in the UK food processing industry. Appl. Therm. Eng. 53, 188–196. https://doi.org/10.1016/j.applthermaleng.2012.03.024

Lorentzen, G., 1995. The use of natural refrigerants: a complete solution to the CFC/HCFC predicament. Int. J. Refrig. 18, 190–197. https://doi.org/10.1016/0140-7007(94)00001-E

Meggers, F., Leibundgut, H., 2010. The potential of wastewater heat and exergy: Decentralized high-temperature recovery with a heat pump. Energy Build. 43, 879–886. https://doi.org/10.1016/j.enbuild.2010.12.008

Nekså, P., 2002. CO2 heat pump systems, in: International Journal of Refrigeration. Elsevier, pp. 421–427. https://doi.org/10.1016/S0140-7007(01)00033-0

Nekså, P., Rekstad, H., Zakeri, G.R., Schiefloe, P.A., 1998. CO2-heat pump water heater: Characteristics, system design and experimental results. Int. J. Refrig. 21, 172–179. https://doi.org/10.1016/S0140-7007(98)00017-6

Pitarch, M., Hervas-Blasco, E., Navarro-Peris, E., Corberán, J.M., 2017a. Exergy analysis on a heat pump working between a heat sink and a heat source of finite heat capacity rate. Int. J. Refrig. 99, 337-350. https://doi.org/10.1016/j.ijrefrig.2018.11.044

Pitarch, M., Hervas-Blasco, E., Navarro-Peris, E., Gonzálvez-Maciá, J., Corberán, J.M., 2017a. Evaluation of optimal subcooling in subcritical heat pump systems. Int. J. Refrig. 78, 18–31. https://doi.org/10.1016/j.ijrefrig.2017.03.015

Pitarch, M., Navarro-Peris, E., Gonzálvez-Maciá, J., Corberán, J.M., 2018. Experimental study of a heat pump with high subcooling in the condenser for sanitary hot water production. Sci. Technol. Built Environ. 24, 105–114. https://doi.org/10.1080/23744731.2017.1333366

Pitarch, M., Navarro-Peris, E., Gonzálvez-Maciá, J., Corberán, J.M., 2017b. Evaluation of different heat pump systems for sanitary hot water production using natural refrigerants. Appl. Energy

190, 911–919. https://doi.org/10.1016/j.apenergy.2016.12.166

Pitarch, M., Navarro-Peris, E., Gonzálvez-Maciá, J., Corberán, J.M., 2016. Experimental study of a subcritical heat pump booster for sanitary hot water production using a subcooler in order to enhance the efficiency of the system with a natural refrigerant (R290). Int. J. Refrig. 73, 226–234. https://doi.org/10.1016/j.ijrefrig.2016.08.017

Pottker, G., Hrnjak, P., 2015. Effect of the condenser subcooling on the performance of vapor compression systems. Int. J. Refrig. 50, 156–164. https://doi.org/10.1016/j.ijrefrig.2014.11.003

Quantum National Distributor, 2018. Commercial Heat Pumps – Quantum [WWW Document]. URL http://quantumenergy.com.au/commercial-heat-pumps/

Shen, C., Lei, Z., Wang, Y., Zhang, C., Yao, Y., 2018. A review on the current research and application of wastewater source heat pumps in China. Therm. Sci. Eng. Prog. https://doi.org/10.1016/j.tsep.2018.03.007

Stene, J., 2007. INTEGRATED CO 2 HEAT PUMP SYSTEMS FOR SPACE HEATING AND HOT WATER HEATING IN LOW-ENERGY HOUSES AND PASSIVE HOUSES. Energy 85, 1–14.

To, E., 2013. W ASTEWATER - - - H EAT R ECOVERY TO H EAT / C OOL B UILDINGS.

Yokoyama, R., Wakui, T., Kamakari, J., Takemura, K., 2010. Performance analysis of a CO2 heat pump water heating system under a daily change in a standardized demand. Energy 35, 718–728. https://doi.org/10.1016/j.energy.2009.11.008

Zehnder, M., 2004. Efficient Air-Water pumps for high temperature lift residential heating, including oil migration aspects. ÉCOLE POLYTECHNIQUE FÉDÉRALE DE LAUSANNE.

LIST OF FIGURES

Figure 1: 0K1V configuration (a) system lay-out (b) refrigerant cycle.....6

Figure 2: Overview of the HP test rig and sensors used in the experimental setup.....9

Figure 3: Heating COP variation with subcooling at different temperatures for both configurations and (a) Tevap_water_inlet=10°C (b) Tevap_water_inlet=20°C and (c) Tevap_water_inlet=30°C. . 13

Figure 4: Compressure suction and discharge pressure variation with subcooling at different water temperatures for the 0K1V and the 10K2V configurations. (a) Tevap_water_inlet=10°C (b) Tevap_water_inlet=20°C and (c) Tevap_water_inlet=30°C. 15

Figure 5: Discharge temperature variation with subcooling at different water temperatures for the 0K1V and the 10K2V configurations. (a) Tevap_water_inlet=10°C (b) Tevap_water_inlet=20°C and (c) Tevap_water_inlet=30°C. 16

Figure 6: COP heating as a function of Tw,co for different water conditions at the inlet of the condenser and evaporator in both configurations. 17

Figure 7: Discharge pressure as a function of Tw,co for different water conditions at the inlet of the condenser and evaporator in both prototypes. 18

Figure 8: Heating COP variation with the water temperature lift at the evaporator. Tw,ci=20˚C and Tw,co=60 ˚C and different Tw,ei for 0K1V and 10K2V configurations. 19

Figure 9: (a) Suction pressure and (b) Suction temperature variation with the water temperature lift at the evaporator. Tw,ci=20˚C and Tw,co=60 ˚C and different Tw,ei for 0K1V and 10K2V configurations..... 20

LIST OF TABLES

Table 2: Characteristics of the components of the HP system..... 9

Table 3: Experimental campaign matrix with 86 measurements carried out in the OK1V configuration 11

Table 4: Experimental campaign matrix with 16 measurements carried out in the OK1V and 10K2V configurations..... 12

Table 5: Experimental campaign matrix with 54 measurements carried out in the OK1V and 10K2V configurations..... 12